ISSN: 2472-3703 DOI: 10.6911/WSRJ.202505_11(5).0006

Research on Complex Power Flow Calculation in Power Systems Using P-Q Decomposition Method Based on POWERWORLD Software

Yingjuan Zheng[1,*] and Guangnu Fu[2]

[1]Wenzhou Polytechnic, Wenzhou Zhejiang, China

[2]State Grid Zhejiang Electric Power Co., Ltd. Longgang Power Supply Company, Longgang Zhejiang, China

[*] Corresponding author

Abstract

According to the three basic requirements of power flow calculation, and following the development of this field, this paper uses the large scale power system visualization software POWERWORLD SIMULATOR, developed by the University of Illinois in the United States to establish the international general power system model, using P-Q decomposition method to calculate the power flow under various operation modes, and the current carrying capacity and voltage level of the line are analyzed. This design focuses on determining the operating state of the whole system, such as voltage (amplitude and phase angle), power distribution and power loss on each bus. This design simulates the power flow of three-machine and nine-node power system. By simulating different running states, the power flow is calculated and compared with the result of MATLAB, and the correctness is verified. Then the different fault schemes are simulated, and the stability calculation is carried out, and the limit cutting time of the fault is calculated. The simulation results can reflect the power distribution intuitively and visually, guarantee the power system safer, steady and economic performance, and raise the economic benefit.

Keywords

Power system; Power flow calculation; P-Q decomposition method; Power distribution; Visual simulation.

1. SIGNIFICANCE AND DEVELOPMENT OF POWER FLOW CALCULATION

Electricity is a key indicator of a country's economic development and an important reflection of the standard of living[1]. It has become an indispensable source of energy and power for modern industrial and agricultural production, transportation, and urban and rural life. The power system, consisting of generation, transmission, transformation, distribution, and consumption, is a large-scale, complex, and real-time entity system.

As early as the 20th century, it was widely recognized that expanding the scale of power systems could bring significant social and economic benefits in energy development, industrial layout, load adjustment, and system safety and economic operation. Consequently, the scale of power systems grew rapidly. With the increasing complexity of power systems, manual calculations became insufficient.

In the mid-1950s, electronic computers were first used for power flow calculations. Since then, various methods have been developed, primarily focusing on the basic requirements of power flow calculation. These requirements can be summarized as follows:

ISSN: 2472-3703 DOI: 10.6911/WSRJ.202505_11(5).0006

(1) Reliability or convergence of the algorithm;

(2) Computational speed and memory usag;

(3) Convenience and flexibility of calculation.

In the early stages of using digital computers to solve power system power flow problems, the Gauss-Seidel iterative method based on the node admittance matrix (referred to as the admittance method) was commonly used. This method was simple in principle and required less memory, making it suitable for the computing technology and power system theory of the time. Later, the impedance matrix-based successive substitution method (referred to as the impedance method) was adopted.

In the early 1960s, with the advent of second-generation digital computers, memory and computational speed improved significantly, enabling the use of the impedance method. The impedance matrix is a full matrix, requiring substantial memory. Each iteration of the impedance method involves computing every element of the impedance matrix, resulting in significant computational effort.

The impedance method[2] improved the convergence of power flow calculations and solved some systems that the admittance method could not. It was widely used and contributed significantly to power system design, operation, and research in China. However, the impedance method's main drawbacks were its large memory usage and computational effort. As systems grew, these drawbacks became more pronounced. To overcome these issues, the block impedance method was developed, which divides a large system into smaller regional systems, reducing memory usage and improving computational speed.

Another approach to overcoming the impedance method's limitations was the Newton-Raphson method[3,4] (referred to as the N-R method). The N-R method, a typical method for solving nonlinear equations in mathematics, linearizes nonlinear equations and has good convergence. Since the power flow calculation problem is based on the admittance matrix, maintaining the sparsity of the coefficient matrix during iterations can significantly improve the efficiency of the N-R method. Since the mid-1960s, with the adoption of optimal ordering elimination, the N-R method surpassed the impedance method in convergence, memory requirements, and computational speed, becoming the widely used method today.

Based on the N-R method, the P-Q decomposition method[5] was developed by focusing on the main characteristics of power systems. The P-Q decomposition method significantly improved computational speed and was quickly adopted.

In the late 1970s, more accurate models, including higher-order terms of the Taylor series, were proposed to improve algorithm performance, leading to the development of nonlinear power flow algorithms. Additionally, to address ill-conditioned power flow problems, the nonlinear programming power flow algorithm[6] was introduced.

Over decades of development, power flow algorithms have matured, and research remains active. With the development of artificial intelligence, genetic algorithms, artificial neural networks, and fuzzy algorithms have been introduced into power flow calculations[7]. However, these new models and algorithms have not yet replaced the Newton and P-Q decomposition methods. As power systems continue to grow, the demand for computational speed increases, and parallel computing technology is expected to play a significant role in power flow calculations.

This paper primarily simulates a three-machine, nine-node system[8] using POWERWORLD software, analyzes the results using MATLAB, and compares the P-Q decomposition method results with the N-R method, MATLAB results, and IEEE9 data to verify correctness. Additionally, the paper simulates different fault scenarios under various operating conditions using POWERWORLD software to perform transient stability calculations and determine the critical

ISSN: 2472-3703 DOI: 10.6911/WSRJ.202505_11(5).0006

fault clearing time. Power flow calculations enable system analysis, making them one of the most fundamental and important calculations in power system analysis, serving as the basis for system safety, economic analysis, real-time control, and dispatch. This has been a long-term research topic for power system researchers.

2. PRINCIPLES AND PROCESS OF POWER FLOW CALCULATION

Power flow calculation mathematically involves solving a set of nonlinear equations[9] that satisfy certain constraints. During the calculation process, or after obtaining results, constraints are used to verify the solution. If the constraints are not met, certain variable values or even the system's operating mode must be modified, and the calculation is repeated.

The results of power flow calculations can be used for power system steady-state studies, security assessments, or optimal power flow analyses, which directly affect the models and methods of power flow calculation. In practice, the Newton-Raphson method and its derivative, the P-Q decomposition method, are primarily used for power flow calculations. The following briefly explains the basic principles of the P-Q decomposition method.

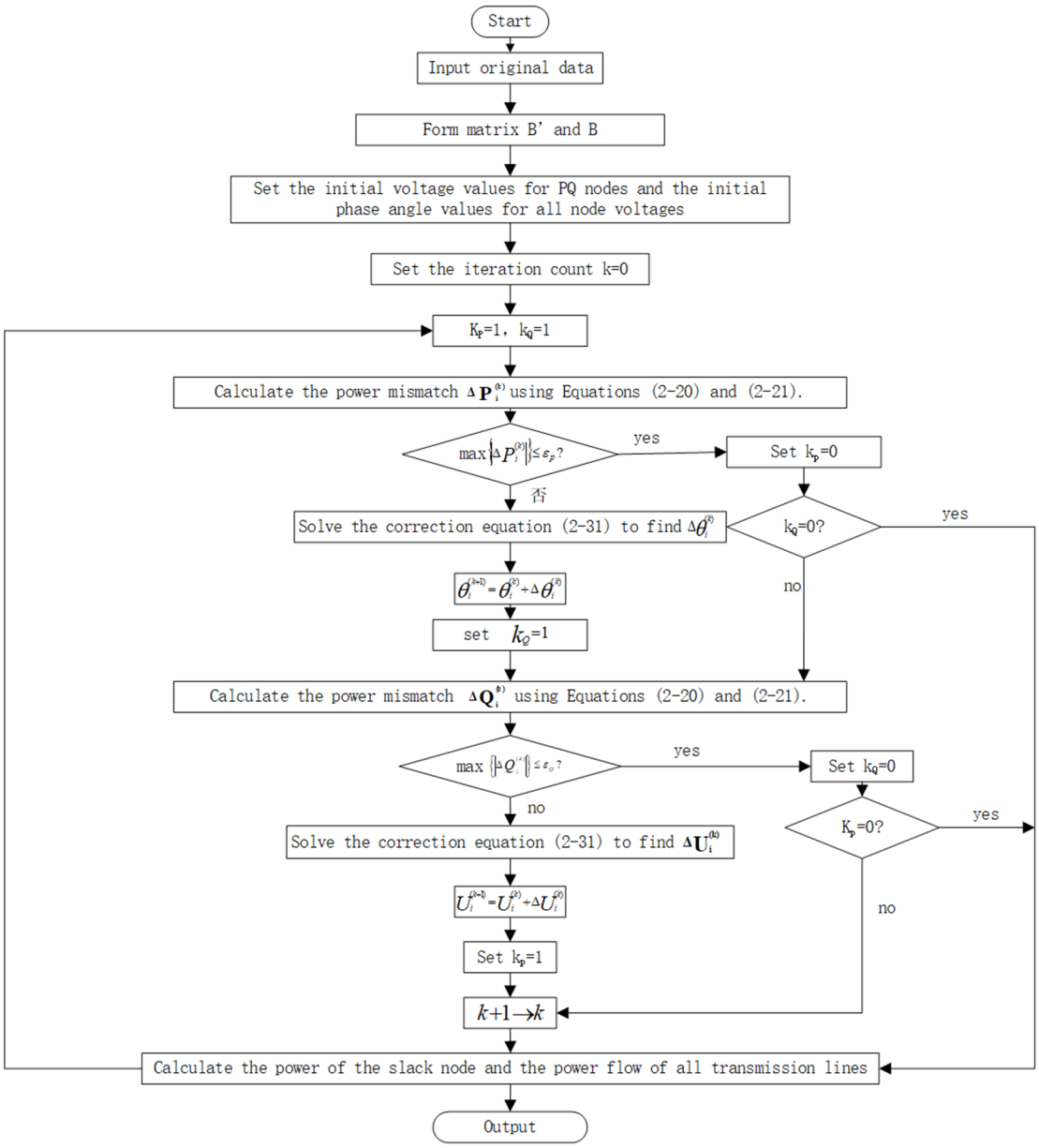

Figure 2.1 Flowchart of the P-Q Decomposition Method

ISSN: 2472-3703 DOI: 10.6911/WSRJ.202505_11(5).0006

The P-Q decomposition method applies the principle of nested loops. Assuming the total number of nodes in the network is n, and m is the sum of PQ nodes and one slack node. The correction equations for active and reactive power are typically of order n−1 and m−1, respectively. However, if node numbering optimization is used, the optimized node numbers cannot be manually determined. A technique is to make both matrices of order n, but set the rows and columns corresponding to the slack node and PV nodes to zero. Another technique is to flag PV nodes, simplifying programming and significantly improving computational speed. The program flowchart is shown in Figure 2.1.

The P-Q decomposition method is derived from the simplified polar form of the Newton-Raphson method. Its basic idea is based on the actual operating characteristics of power systems: typically, the reactance of the network is much larger than the resistance, so small changes in bus voltage magnitude ΔV have little effect on active power ΔP. Similarly, small changes in bus voltage phase angle Δθ do not significantly affect reactive power ΔQ. Therefore, when the node power equations are expressed in polar form, the correction equations can be simplified as:

$$\begin{bmatrix} \Delta P \\ \Delta Q \end{bmatrix} = \begin{bmatrix} H & 0 \\ 0 & L \end{bmatrix} \begin{bmatrix} \Delta \theta \\ \Delta V / V \end{bmatrix} \tag{2-1}$$

This reduces the 2(n−1) order linear equations to two n−1 order linear equations, separating P and Q for iterative calculation, significantly reducing computational effort. However, L still change during iterations and are asymmetric matrices. The key simplification of the Newton method is to make the coefficient matrices in the correction equations constant symmetric matrices during iterations.

In general, the phase angle difference θ_{ij} between the voltages at the two ends of a line is small (not exceeding 10° to 20°). Therefore, it can be assumed that:

$$\left.\begin{aligned} \cos\theta_{ij} &\approx 1 \\ G_{ij}\sin\theta_{ij} &<< B_{ij} \end{aligned}\right\} \tag{2-2}$$

Additionally, the admittance B^{LDi} corresponding to the reactive power at each node is much smaller than the imaginary part of the node's self-admittance, i.e.,

$$B_{LDi} = \frac{Q_i}{V_i^2} << B_{ii}$$

Thus,

$$Q_i << V_i^2 B_{ii} \tag{2-3}$$

Considering these relationships, the elements of the coefficient matrices in the correction equations can be expressed as:

$$H_{ij} = V_i V_j B_{ij} \qquad \text{(i,j=1,2,……, n-1)} \tag{2-4}$$

$$L_{ij} = V_i V_j B_{ij} \qquad \text{(i,j=1,2,……, m)} \tag{2-5}$$

ISSN: 2472-3703 DOI: 10.6911/WSRJ.202505_11(5).0006

The coefficient matrices H and L can be written as:

$$H=\begin{bmatrix} V_1B_{11}V_1 & V_1B_{12}V_2\cdots\cdots V_1B_{1,n-1}V_{n-1} \\ V_2B_{21}V_1 & V_2B_{22}V_2\cdots\cdots V_2B_{2,n-1}V_{n-1} \\ \vdots & \vdots \\ \vdots & \vdots \\ V_{n-1}B_{n-1,1}V_1 & V_{n-1}B_{n-1,2}V_2\cdots\cdots V_{n-1}B_{n-1,n-1}V_{n-1} \end{bmatrix}$$

$$=\begin{bmatrix} V_1 & & & \\ & V_2 & & \\ & & \cdots & \\ & & & V_{n-1} \end{bmatrix}\begin{bmatrix} B_{11} & B_{12}\cdots\cdots\cdots B_{1,n-1} \\ B_{21} & B_{22}\cdots\cdots\cdots B_{2,n-1} \\ \vdots & \\ B_{n-1,1} & B_{n-1,2}\cdots\cdots B_{n-1,n-1} \end{bmatrix}\begin{bmatrix} V_1 & & & \\ & V_2 & & \\ & & \cdots & \\ & & & V_{n-1} \end{bmatrix}$$

$$=V_{D1}BV_{D1} \tag{2-6}$$

$$L=\begin{bmatrix} V_1B_{11}V_1 & V_1B_{12}V_2\cdots\cdots\cdots V_1B_{1m}V_m \\ V_2B_{21}V_1 & V_2B_{22}V_2\cdots\cdots\cdots V_2B_{2m}V_m \\ \vdots & \vdots \\ V_mB_{m1}V_m & V_mB_{m2}V_2\cdots\cdots\cdots V_mB_{mm}V_m \end{bmatrix}$$

$$=\begin{bmatrix} V_1 & & & \\ & V_2 & & \\ & & \cdots & \\ & & & V_m \end{bmatrix}\begin{bmatrix} B_{11} & B_{12} & \cdots\cdots\cdots & B_{1m} \\ B_{21} & B_{22} & \cdots\cdots\cdots & B_{2m} \\ \vdots & \vdots & & \vdots \\ B_{m1} & B_{m2} & \cdots\cdots\cdots & B_{mm} \end{bmatrix}\begin{bmatrix} V_1 & & & \\ & V_2 & & \\ & & \cdots & \\ & & & V_m \end{bmatrix}$$

$$=V_{D2}B''V_{D2} \tag{2-7}$$

Substituting these into the correction equations, we get:

$$[\Delta P]=-[V_{D1}][B'][V_{D1}][\Delta\theta]$$
$$[\Delta Q]=-[V_{D2}][B'']\Delta V]$$

Multiplying both sides by $[V_{D1}]^{-1}$ and $[V_{D2}]^{-1}$, respectively, we obtain:

$$[V_{D1}]^{-1}[\Delta P]=-[B'][V_{D1}][\Delta\theta] \tag{2-8}$$

$$[V_{D2}]^{-1}[\Delta Q]=-[B'']\Delta V] \tag{2-9}$$

These are the simplified correction equations, which can be expanded as:

ISSN: 2472-3703 DOI: 10.6911/WSRJ.202505_11(5).0006

$$\begin{bmatrix} \frac{\Delta P_1}{V_1} \\ \frac{\Delta P_2}{V_2} \\ \vdots \\ \frac{\Delta P_{n-1}}{V_{n-1}} \end{bmatrix} = -\begin{bmatrix} B_{11} & B_{12} & \cdots\cdots & B_{1,n-1} \\ B_{21} & B_{22} & \cdots\cdots & B_{2,n-1} \\ \vdots & \vdots & & \vdots \\ B_{n-1,1} & B_{n-1,2} & & \cdots\cdots B_{n-1,n-1} \end{bmatrix} \begin{bmatrix} V_1\Delta\theta_1 \\ V_2\Delta\theta_2 \\ \vdots \\ V_{n-1}\Delta\theta_{n-1} \end{bmatrix} \tag{2-10}$$

$$\begin{bmatrix} \frac{\Delta Q_1}{V_1} \\ \frac{\Delta Q_2}{V_2} \\ \vdots \\ \frac{\Delta Q_m}{V_m} \end{bmatrix} = -\begin{bmatrix} B_{11} & B_{12} & \cdots\cdots\cdots & B_{1m} \\ B_{21} & B_{22} & \cdots\cdots\cdots & B_{2m} \\ \vdots & \vdots & & \vdots \\ B_{m1} & B_{m2} & \cdots\cdots\cdots & B_{mm} \end{bmatrix} \begin{bmatrix} \Delta V_1 \\ \Delta V_2 \\ \vdots \\ \Delta V_m \end{bmatrix} \tag{2-11}$$

In these correction equations, the coefficient matrix elements are the imaginary parts of the system admittance matrix, making the coefficient matrices symmetric and constant during iterations, significantly reducing computational effort.

The node power increments in polar form are:

$$\begin{aligned} \Delta P_i &= P_{is} - V_i \sum_{j=1}^{n} V_j (G_{ij}\cos\theta_{ij} + B_{ij}\sin\theta_{ij}) = 0 \\ \Delta Q_i &= Q_{is} - V_i \sum_{j=1}^{n} V_j (G_{ij}\sin\theta_{ij} - B_{ij}\cos\theta_{ij}) = 0 \end{aligned} \tag{2-12}$$

Equations (2-10), (2-11), and (2-12) form the basic equations of the P-Q decomposition method iterative process.

Based on the node admittance matrix, in an n-node power network, the power flow equations generally include four variables: P, Q, V, and δ. From the actual operation of power systems, nodes can be divided into three types:

PQ Nodes: In these nodes, active power P and reactive power Q are known, while the voltage magnitude is unknown. Typically, substations use this type of node since they lack generation equipment, and their generation power is usually zero. Some power plants with fixed output power over a certain period also use PQ nodes. Therefore, most nodes in power systems are PQ nodes.

PV Nodes: In these nodes, active power P and voltage magnitude V are known, while reactive power Q and phase angle δ need to be calculated. These nodes are also known as voltage control nodes since they maintain a given voltage magnitude with sufficient adjustable reactive power. PV nodes are typically used in power plants with reactive power reserves and substations with adjustable reactive power sources, but they are less common in power systems.

Slack Node: Before the power flow calculation results are obtained, the power loss in the network is unknown. Therefore, at least one node's active power P cannot be determined. This node, which balances the active power of the system, is called the slack node. The slack node's active and reactive power are usually calculated. The slack node is typically used in the main frequency control power plant. However, there are two special cases: (1) to improve the

ISSN: 2472-3703 DOI: 10.6911/WSRJ.202505_11(5).0006

convergence of the admittance matrix method, the power plant with the most outgoing lines can be used as the slack node; (2) for regional power grid calculations, the largest power source outgoing line can be used as the slack node.

Among the four operating parameters P, Q, V, δ of these three types of nodes, two are known, and two are to be determined, differing only in type. Additionally, the node numbering order affects the convenience of power flow calculation, mainly by reducing the workload of node optimization and improving optimization effectiveness, thereby speeding up the calculation. Optimization methods include static optimization, semi-dynamic optimization, and dynamic optimization. Among these, static optimization is the simplest but least effective, while dynamic optimization is the most effective but computationally intensive. Therefore, semi-dynamic node numbering optimization is commonly used. The basic idea of semi-dynamic optimization is to number the nodes with the fewest connected branches first, then eliminate that node. Each elimination changes the number of connected branches for the remaining nodes, and the process repeats until all nodes are numbered. The effect of admittance matrix elimination is similar to simplifying a network from a star to a multi-triangle configuration.

Table 2.1 Comparison of Common Power System Node Types

Node Type	P	Q	U	δ
PQ Node	√	√		
PV Node	√		√	
Balancing node			√	√

In addition to node types, power system operation must meet certain technical and economic requirements. These requirements form the constraints on certain variables in the power flow problem. Common constraints include:

①Node Voltage Constraint: The node voltage should be less than the maximum rated voltage and greater than the minimum rated voltage, i.e.,

$$V_{i\min} \le V_i \le V_{i\max} \qquad (i = 1, 2, \cdots n) \tag{2-13}$$

From the perspective of ensuring power quality and supply security, all electrical equipment in the power system must operate near the rated voltage. The voltage magnitude of PV nodes must be given according to this condition. Therefore, this constraint applies to PQ nodes.

②Node Power Constraint: The active and reactive power of nodes should be less than the maximum rated power and greater than the minimum rated power, i.e.,

$$\begin{cases} P_{Gi\min} \le P_{Gi} \le P_{Gi\max} \\ Q_{Gi\min} \le Q_{Gi} \le Q_{Gi\max} \end{cases} \tag{2-14}$$

The active and reactive power of PQ nodes, as well as the active power of PV nodes, must satisfy these conditions when given. Therefore, the active and reactive power of the slack node and the reactive power of PV nodes should be checked against these conditions.

③Voltage Phase Difference Constraint: The voltage phase difference between nodes should be less than the minimum rated phase difference, i.e.,

$$|\theta_{ij}| = |\theta_i - \theta_j| < |\theta_i - \theta_j|_{\max} \tag{2-15}$$

ISSN: 2472-3703 DOI: 10.6911/WSRJ.202505_11(5).0006

To ensure system stability, the voltage phase difference across certain transmission lines should not exceed a certain value. This constraint is primarily significant for this purpose.

3. P-Q DECOMPOSITION METHOD POWER FLOW CALCULATION BASED ON POWERWORLD

3.1. Three-Machine, Nine-Node System Under Different Operating Conditions

Based on the international standard nine-node system, a project is established by adding components, setting relevant parameters, and adjusting the appearance. The resulting three-machine, nine-node system (referred to as State 1) is shown in Figure 3.1, consisting of 9 nodes, 9 AC lines, 3 generators, and 3 loads. The P-Q decomposition method is used to simulate the power flow under this model. The initial parameters of each node are shown in Table 3.1.

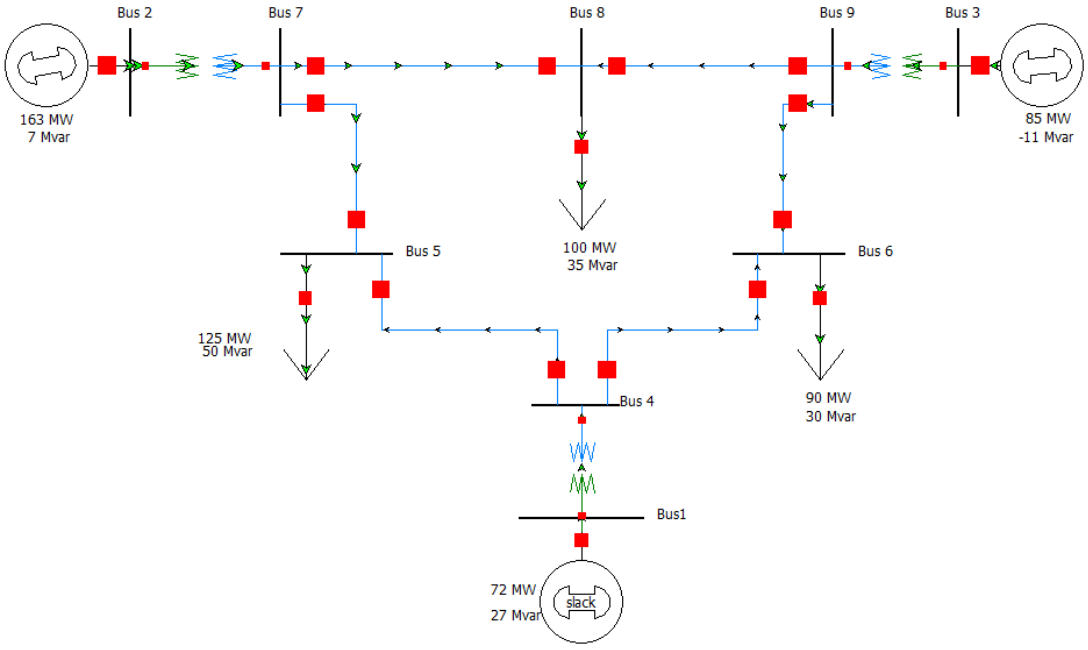

Figure 3.1 Single-Line Diagram of the Three-Machine, Nine-Node System in State 1

Table 3.1 Initial Parameters for Operating State 1

Node	Base Voltage	Per Unit Voltage	Phase Angle	Active Power Load	Reactive Power Load	Generator Active Power	Generator Reactive Power
Bus1	16.5	1.04	0			71.64	27.04
Bus2	18	1.025	9.28			163	6.65
Bus3	13.8	1.025	4.67			85	-10.86
Bus5	230	0.99564	-3.99	125	50		
Bus6	230	1.01266	-3.69	90	30		
Bus8	230	1.01589	0.73	100	35		
Bus4	230	1.02579	-2.22				
Bus7	230	1.02577	3.72				
Bus9	230	1.03236	1.97				

To simulate load shedding during power system operation[10], the load connected to Bus 5 is removed during stable operation. After a brief wait, the system returns to stable operation

ISSN: 2472-3703 DOI: 10.6911/WSRJ.202505_11(5).0006

(referred to as State 2). The system load decreases, and the active and reactive power at Node 5 become zero, but it remains a PQ node. The system parameters are shown in Table 3.2.

Table 3.2 Parameters for Operating State 2

Node	Base Voltage	Per Unit Voltage	Phase Angle	Active Power Load	Reactive Power Load	Generator Active Power	Generator Reactive Power
Bus1	16.5	1.04	0			-53.09	1.15
Bus2	18	1.025	16.58			163	-13.61
Bus3	13.8	1.025	10.71			85	-18.9
Bus5	230	1.03978	1.62	0	0		
Bus6	230	1.047	4.74	90	30		
Bus8	230	1.02259	0.96				
Bus4	230	1.03807	11.09				
Bus7	230	1.02499	7.59	100	35		
Bus9	230	1.03695	8.02				

Similarly, during stable operation (State 1), the generator connected to Bus 3 is removed. After the system returns to stable operation, a new state (referred to as State 3) is obtained. In this state, the system's output decreases, and Node 3 no longer outputs power, changing from a PV node to a PQ node. The power flow parameters are shown in Table 3.3.

Table 3.3 Parameters for Operating State 3

Node	Base Voltage	Per Unit Voltage	Phase Angle	Active Power Load	Reactive Power Load	Generator Active Power	Generator Reactive Power
Bus1	16.5	1.04	0			155.63	22.93
Bus2	18	1.025	2.11			163	3.19
Bus3	13.8	1.0385	-8.35			0	0
Bus5	230	1.03091	-4.8				
Bus6	230	1.00276	-8.09	125	50		
Bus8	230	1.02001	-8.94	90	30		
Bus4	230	1.02787	-3.44				
Bus7	230	1.01895	-7.74	100	35		
Bus9	230	1.0385	-8.35				

The above are the power flow calculation results under three operating conditions. It can be observed that under different operating conditions, the voltage magnitude and phase angle of Node 1 remain constant, serving as the slack node; the active power output and voltage magnitude of Node 2 remain constant, serving as a PV node; and the active and reactive power loads of Nodes 6 and 8 remain constant, serving as PQ nodes.

3.2. Fault Scenario Settings for the Three-Machine, Nine-Node System

The ability of a power system to withstand disturbances without experiencing loss of synchronism, frequency collapse, or voltage collapse is essential for ensuring normal operation. From a narrow perspective, power system stability refers specifically to the avoidance of loss of synchronism, meaning that all AC synchronous generators in the system must remain

ISSN: 2472-3703 DOI: 10.6911/WSRJ.202505_11(5).0006

synchronized during disturbances, regardless of the number of generators or the size of the interconnected network. From a broader perspective, power system stability also includes the system's ability to recover synchronism after entering an asynchronous state, provided certain conditions are met. This capability is known as comprehensive stability[11].

To verify that the three-machine, nine-node system possesses sufficient stability, this study selects 2–3 fault scenarios and uses POWERWORLD software for stability calculations. The goal is to test whether the system can autonomously recover stability, determine the swing duration, and calculate the critical fault clearing time.

Before performing transient stability calculations, the generator model, excitation system model, governor model, and stabilizer model for the generator connected to Node 1 are configured. After setting up the dynamic models, simulation settings are adjusted, with the simulation time set to 0–40 seconds. A three-phase short-circuit fault is applied to Bus 5 at 1 second (referred to as Fault 1). The latest time to clear the fault[12] while maintaining system stability is determined. The generator power angles are selected for output, as shown in Figure 3.2. Table 3.5 presents the critical fault clearing time data obtained using the bisection method.

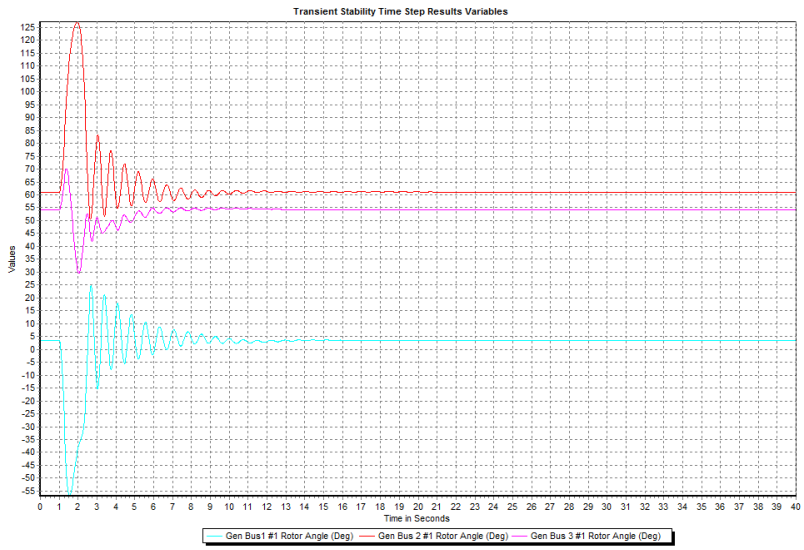

(a)

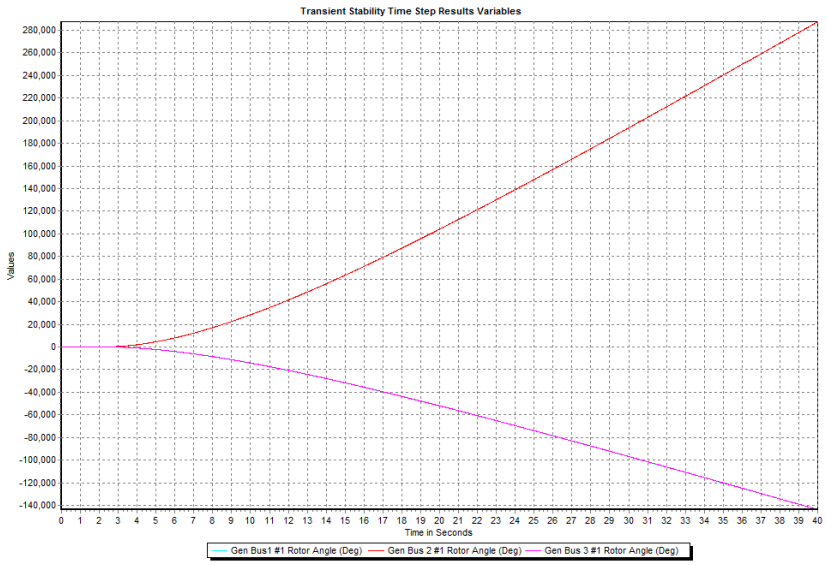

(b)

Figure 3.2 Generator Power Angle Curves

ISSN: 2472-3703 DOI: 10.6911/WSRJ.202505_11(5).0006

Table 3.5 Critical Fault Clearing Time Data

Fault Clearing Time (s)	1.1000	1.5000	1.3000	1.2000	1.2500	1.5750
System Stability	Stable	Unstable	Unstable	Stable	Stable	Unstable
Fault Clearing Time (s)	1.4125	1.3313	1.2907	1.2704	1.2806	1.2856
System Stability	Unstable	Unstable	Unstable	Stable	Stable	Stable
Fault Clearing Time (s)	1.2881	1.2869	1.2875	1.2878	1.2879	1.2880
System Stability	Unstable	Stable	Stable	Stable	Stable	Stable

From the data in the table, it can be concluded that after a three-phase short-circuit fault occurs at Bus 5, clearing the fault within 0.2880 seconds ensures that the system autonomously recovers stability, as shown in Figure 3.2(a). The initial power angle of the generator is approximately 4°, and the system returns to steady-state operation after about 10 seconds. If the fault is cleared at 0.2881 seconds or later, the system loses stability, as shown in Figure 3.2(b).

The dynamic models for the generators connected to Node 1, Node 2, and Node 3 are configured. Similarly, a three-phase short-circuit fault is applied to Bus 5 at 1 second (referred to as Fault 2). The goal is to determine the latest time to clear the fault while ensuring that the system can autonomously recover stability. The generator power angles are selected for output, as shown in Figure 3.3. Table 3.6 presents the critical fault clearing time data obtained using the bisection method.

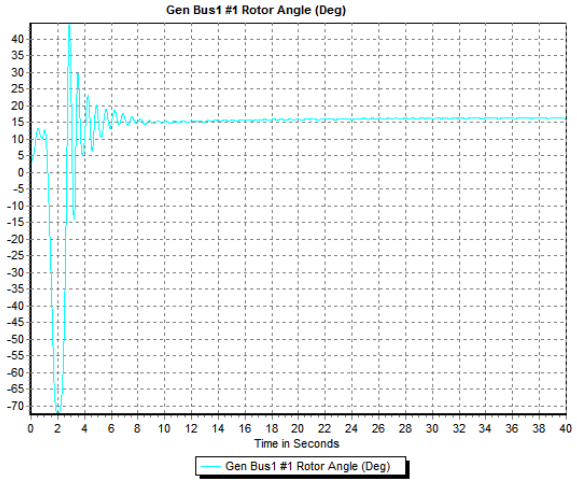

(a)

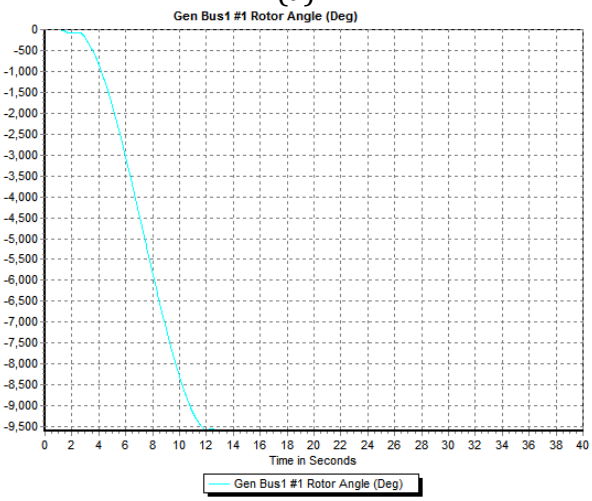

(b)

Figure 3.3 Generator Swing Curves

ISSN: 2472-3703 DOI: 10.6911/WSRJ.202505_11(5).0006

Table 3.6 Critical Fault Clearing Time Data

Fault Clearing Time (s)	2	1.5	1.75	1.625	1.6875	1.6563
System Stability	Unstable	Stable	Unstable	Stable	Unstable	Stable
Fault Clearing Time (s)	1.6712	1.6638	1.6675	1.6694	1.6685	1.668
System Stability	Unstable	Stable	Stable	Stable	Unstable	Stable
Fault Clearing Time (s)	1.6683	1.66815	1.66808	1.66812	1.6681	
System Stability	Unstable	Unstable	Stable	Unstable	Stable	

From the data in the table, it can be observed that for the same fault scenario, when all three generators (connected to Nodes 1, 2, and 3) participate in frequency regulation, the system can withstand the fault for a longer duration without collapsing compared to when only one generator is regulating frequency. This demonstrates the enhanced stability provided by multiple generators working in coordination during fault conditions.

The critical fault clearing time for this scenario is determined to be approximately 1.66810 seconds, beyond which the system loses stability. This analysis highlights the importance of coordinated generator response in maintaining system stability during faults.

4. COMPARISON OF POWER FLOW CALCULATION RESULTS

Table 4.1 Comparison of Voltage Magnitude and Phase Angle Results for State 1

Node	**Base Voltage**	**Per Unit Voltage**			
		MATLAB	**P-Q**	**N-R**	**Standard**
Bus 1	16.5	1.04	1.04	1.04	1.04
Bus 2	18	1.025	1.025	1.025	1.025
Bus 3	13.8	1.025	1.025	1.025	1.025
Bus 4	230	1.0258	1.02579	1.02579	1.025
Bus 5	230	0.9956	0.99564	0.99564	0.995
Bus 6	230	1.0127	1.01266	1.01266	1.012
Bus 7	230	1.0258	1.02577	1.02577	1.025
Bus 8	230	1.0159	1.01589	1.01589	1.015
Bus 9	230	1.0324	1.03236	1.03236	1.032
Node	**Base Voltage**	**Phase Angle**			
		MATLAB	**P-Q**	**N-R**	**Standard**
Bus 1		0	0	0	0
Bus 1	16.5	9.28	9.28	9.28	9.28
Bus 2	18	4.6647	4.67	4.67	4.6647
Bus 3	13.8	-2.2168	-2.22	-2.22	-2.216
Bus 4	230	-3.9888	-3.99	-3.99	-3.988
Bus 5	230	-3.6874	-3.69	-3.69	-3.687
Bus 6	230	3.7197	3.72	3.72	3.7197
Bus 7	230	0.7275	0.73	0.73	0.7275
Bus 8	230	1.9667	1.97	1.97	1.9667

ISSN: 2472-3703 DOI: 10.6911/WSRJ.202505_11(5).0006

In addition to performing power flow calculations for the three operating conditions of the three-machine, nine-node power system in POWERWORLD, I also conducted power flow calculations for the same system using MATLAB, employing both the P-Q decomposition method and the Newton-Raphson (N-R) method. Below, the simulation results are compared with standard test cases for data analysis.

The results from POWERWORLD using the P-Q decomposition method are compared with those from the N-R method and MATLAB's P-Q decomposition method. These comparisons are supplemented with standard test cases to validate the correctness of the three-machine, nine-node system, facilitating further longitudinal analysis. The power flow calculation data are presented in Tables 4.1 and 4.2:

Table 4.2 Comparison of Power Distribution Results for State 1

From Node	To Node	Active Power			Reactive Power		
		MATLAB	P-Q	N-R	MATLAB	P-Q	N-R
Bus 4	Bus 1	-0.7164	-71.6	-71.6	-0.2393	-23.9	-23.9
Bus 2	Bus 7	1.6300	163	163	0.0666	6.6	6.6
Bus 9	Bus 3	-0.8500	-85	-85	0.1495	15	15
Bus 5	Bus 4	-0.4068	-40.7	-40.7	-0.3869	-38.7	-38.7
Bus 6	Bus 4	-0.3054	-30.5	-30.5	-0.1655	-16.5	-16.5
Bus 7	Bus 5	0.8662	86.6	86.6	-0.0838	-8.4	-8.4
Bus 9	Bus 6	0.6082	60.8	60.8	-0.1807	-18.1	-18.1
Bus 7	Bus 8	0.7638	76.4	76.4	-0.0080	-0.8	-0.8
Bus 8	Bus 9	-0.2410	-24.1	-24.1	-0.2430	-24.3	-24.3
From Node	To Node	Active Power Loss			Reactive Power Loss		
		MATLAB	P-Q	N-R	MATLAB	P-Q	N-R
Bus 4	Bus 1	0.0000	0	0	0.0312	3.12	3.12
Bus 2	Bus 7	0.0000	0	0	0.1583	15.83	15.83
Bus 9	Bus 3	0.0000	0	0	0.0410	4.1	4.1
Bus 5	Bus 4	0.0026	0.26	0.26	-0.1579	-15.79	-15.79
Bus 6	Bus 4	0.0017	0.17	0.17	-0.1551	-15.51	-15.51
Bus 7	Bus 5	0.0230	2.3	2.3	-0.1969	-19.69	-19.69
Bus 9	Bus 6	0.0135	1.35	1.35	-0.3153	-31.53	-31.53
Bus 7	Bus 8	0.0048	0.48	0.48	-0.1150	-11.5	-11.5
Bus 8	Bus 9	0.0009	0.09	0.09	-0.2118	-21.18	-21.18

From the data in State 1, it is evident that the three-machine, nine-node system modeled in POWERWORLD, whether using the P-Q decomposition method or the Newton-Raphson method, produces results that match those obtained from MATLAB. Furthermore, when compared with the standard test cases, the errors are minimal and negligible. The per unit voltage errors are controlled within 0.001, corresponding to actual voltage errors of less than 0.1 kV, and the phase angle errors are within 0.01°. The following sections provide similar comparisons for State 2 and State 3, with the data presented in Tables 4.3–4.6.

ISSN: 2472-3703 DOI: 10.6911/WSRJ.202505_11(5).0006

Table 4.3 Comparison of Voltage Magnitude and Phase Angle Results for State 2

Node	Base Voltage	Per Unit Voltage			Phase Angle		
		MATLAB	P-Q Method	N-R Method	MATLAB	P-Q Method	N-R Method
Bus 1	16.5	1.04	1.04	1.04	0	0	0
Bus 2	18	1.025	1.025	1.025	16.5828	16.58	16.58
Bus 3	13.8	1.025	1.025	1.025	10.7048	10.71	10.71
Bus 4	230	1.0398	1.03978	1.03978	1.6205	1.62	1.62
Bus 5	230	1.047	1.047	1.047	4.7373	4.74	4.74
Bus 6	230	1.0226	1.02259	1.02259	0.9585	0.96	0.96
Bus 7	230	1.0381	1.03807	1.03807	11.0886	11.09	11.09
Bus 8	230	1.025	1.02499	1.02499	7.5896	7.59	7.59
Bus 9	230	1.0369	1.03695	1.03695	8.0188	8.02	8.02

Table 4.4 Comparison of Power Distribution Results for State 2

From Node	To Node	Active Power			Reactive Power		
		MATLAB	P-Q Method	N-R Method	MATLAB	P-Q Method	N-R Method
Bus 4	**Bus 1**	0.5309	53.1	53.1	0.0034	0.3	0.3
Bus 2	**Bus 7**	1.6300	163	163	-0.1361	-13.6	-13.6
Bus 9	**Bus 3**	-0.8500	-85	-85	0.2313	23.1	23.1
Bus 5	**Bus 4**	0.6994	69.9	69.9	-0.0708	-7.1	-7.1
Bus 6	**Bus 4**	-0.1631	-16.3	-16.3	-0.2428	-24.3	-24.3
Bus 7	**Bus 5**	0.7153	71.5	71.5	-0.3232	-32.3	-32.3
Bus 9	**Bus 6**	0.7577	75.8	75.8	-0.2314	-23.1	-23.1
Bus 7	**Bus 8**	0.9147	91.5	91.5	0.0279	2.8	2.8
Bus 8	**Bus 9**	-0.0920	-9.2	-9.2	-0.2202	-22	-22
From Node	**To Node**	**Active Power Loss**			**Reactive Power Loss**		
		MATLAB	P-Q Method	N-R Method	MATLAB	P-Q Method	N-R Method
Bus 4	**Bus 1**	0.0000	0	0	0.0150	1.5	1.5
Bus 2	**Bus 7**	0.0000	0	0	0.1592	15.92	15.92
Bus 9	**Bus 3**	0.0000	0	0	0.0423	4.23	4.23
Bus 5	**Bus 4**	0.0045	0.45	0.45	-0.1536	-15.36	-15.36
Bus 6	**Bus 4**	0.0008	0.08	0.08	-0.1634	-16.34	-16.34
Bus 7	**Bus 5**	0.0159	1.59	1.59	-0.2524	-25.24	-25.24
Bus 9	**Bus 6**	0.0209	2.09	2.09	-0.2886	-28.86	-28.86
Bus 7	**Bus 8**	0.0067	0.67	0.67	-0.1019	-10.19	-10.19
Bus 8	**Bus 9**	0.0002	0.02	0.02	-0.2202	-22.02	-22.02

ISSN: 2472-3703 DOI: 10.6911/WSRJ.202505_11(5).0006

Table 4.5 Comparison of Voltage Magnitude and Phase Angle Results for State 3

Node	Base Voltage	Per Unit Voltage			Phase Angle		
		MATLAB	P-Q Method	N-R Method	MATLAB	MATLAB	P-Q Method
Bus 1	16.5	1.04	1.04	1.04	0	0	0
Bus 2	18	1.025	1.025	1.025	2.1108	2.11	2.11
Bus 3	13.8	1.0385	1.0385	1.0385	-8.3469	-8.35	-8.35
Bus 4	230	1.0309	1.03091	1.03091	-4.7961	-4.8	-4.8
Bus 5	230	1.0027	1.00276	1.00276	-8.0875	-8.09	-8.09
Bus 6	230	1.02	1.02001	1.02001	-8.9389	-8.94	-8.94
Bus 7	230	1.0279	1.02787	1.02787	-3.4382	-3.44	-3.44
Bus 8	230	1.0189	1.01895	1.01895	-7.7415	-7.74	-7.74
Bus 9	230	1.0385	1.0385	1.0385	-8.3469	-8.35	-8.35

Table 4.6 Comparison of Power Flow Calculation Results for State 3.

From Node	To Node	Active Power			Reactive Power		
		MATLAB	P-Q Method	N-R Method	MATLAB	P-Q Method	N-R Method
Bus 4	**Bus 1**	-1.5563	-155.6	-155.6	-0.0977	-9.7	-9.7
Bus 2	**Bus 7**	1.6300	163	163	0.0320	3.2	3.2
Bus 9	**Bus 3**	0.0000	0	0	0.0000	0	0
Bus 5	**Bus 4**	-0.7249	-72.5	-72.5	-0.3153	-31.5	-31.5
Bus 6	**Bus 4**	-0.8147	-81.5	-81.5	-0.0228	-2.3	-2.3
Bus 7	**Bus 5**	0.5339	53.4	53.4	-0.0864	-8.6	-8.6
Bus 9	**Bus 6**	0.0859	8.6	8.6	-0.0994	-9.9	-9.9
Bus 7	**Bus 8**	1.0961	109.6	109.6	-0.0397	-4	-4
Bus 8	**Bus 9**	0.0864	8.6	8.6	-0.3157	-31.6	-31.6
From Node	**To Node**	**Active Power Loss**			**Reactive Power Loss**		
		MATLAB	P-Q Method	N-R Method	MATLAB	P-Q Method	N-R Method
Bus 4	**Bus 1**	0.0000	0	0	0.1318	13.18	13.18
Bus 2	**Bus 7**	0.0000	0	0	0.1581	15.81	15.81
Bus 9	**Bus 3**	0.0000	0	0	0.0000	0	0
Bus 5	**Bus 4**	0.0057	0.57	0.57	-0.1332	-13.32	-13.32
Bus 6	**Bus 4**	0.0109	1.09	1.09	-0.1071	-10.71	-10.71
Bus 7	**Bus 5**	0.0088	0.88	0.88	-0.2712	-27.12	-27.12
Bus 9	**Bus 6**	0.0006	0.06	0.06	-0.3767	-37.67	-37.67
Bus 7	**Bus 8**	0.0097	0.97	0.97	-0.0741	-7.41	-7.41
Bus 8	**Bus 9**	0.0006	0.06	0.06	-0.2163	-21.63	-21.63

Whether analyzing data from operating state 1, state 2, or state 3, it can be concluded that the three-machine nine-bus system built using POWERWORLD software achieves highly accurate power flow calculations, whether using the P-Q decomposition method or the Newton-Raphson

ISSN: 2472-3703 DOI: 10.6911/WSRJ.202505_11(5).0006

method. The results match those obtained from MATLAB with minimal errors, which are negligible. This demonstrates the robust power flow calculation capabilities of POWERWORLD software. Additionally, it offers a unique feature not commonly found in other power flow calculation software—visualization, making it a powerful learning tool for beginners in power systems.

5. CONCLUSION

In this paper, the use of POWERWORLD simulation software to conduct detailed power flow analysis on the classic three-machine nine-bus system has not only enabled the intuitive identification of which lines can be safely disconnected without compromising overall system stability but also facilitated in-depth observation and assessment of the potential impacts and risks associated with component switching on the entire power system. The research demonstrates that such simulation experiments offer a vivid, dynamic, and efficient approach to deepening the understanding of fundamental principles of power system operation, particularly concerning how electricity trading policies influence system safety, economy, and reliability.

In summary, leveraging simulation tools like POWERWORLD for power system analysis is crucial for ensuring economical, safe, and stable power system operations and provides valuable guidance for the renovation and reinforcement of power networks. Moreover, this method not only enhances educational objectives by helping students and researchers better comprehend the complex mechanisms of power systems but also exhibits practical value in actual power system management and optimization. Future work will further explore the application potential of these simulation techniques to address increasingly complex challenges in power systems and support smarter and more sustainable grid development.

ACKNOWLEDGMENTS

This paper was supported by the Wenzhou Polytechnic 's Higher Vocational Education Special Research Project on 'Integrating Enterprises into Schools and Jointly Cultivating Talents by Schools and Enterprises'—an exploration of talent cultivation models for new energy equipment technology (Fund Number: WZYGJzd202302). We hereby express our sincere gratitude for this support.

REFERENCES

[1] Xue Jing(2024) : A New Perspective on Power Supply and Demand Analysis in the New Power System [J] , China Electric Power Enterprise Management.

[2] Sun Qiuye: Power System Analysis [M] , Posts & Telecom Press.

[3] Zhang Feng(2009) : Convergence Analysis of Power Flow Calculation in Systems with Small Impedance [D].

[4] Liu Dan(2025) : Research on Classic Algorithms for Power System Optimization [D].

[5] Yao Yubin, Cai Xingguo and Chen Xueyun(2000): Convergence Analysis of PQ Decomposition Method for Power Flow Calculation in Systems with Small Impedance Branches [J].

[6] Wan Li and Yuan Rongxiang(2005) : Review of Optimal Power Flow Algorithms [J].

[7] Zhong Bo(2004), Research on Reliability Evaluation Models and Algorithms of Power Systems Based on Soft Computing Theory [D].

[8] Shi Zhiping(2011) : Dynamic Stability Analysis of Power Systems Based on Three-Machine Nine-Bus Model [J].

ISSN: 2472-3703 DOI: 10.6911/WSRJ.202505_11(5).0006

[9] Li Yining, Wu Hao and Xin Huanhai (2015) : Stochastic Power Flow of Power Systems Based on Generalized Polynomial Chaos Method [J].

[10] Zhu Runlin(2021) : Modeling of Impact Load in Power Systems and Its Impact on Voltage Stability Analysis [D].

[11] Sun Huadong, Tang Yong and Ma Shiying(2006) : Review on Definitions and Classification of Power System Stability [J].

[12] Zhang Lixiao(2014) : Research on Reliability and Condition-Based Maintenance of Relay Protection [D].